bioRxiv preprint doi: https://doi.org/10.1101/2021.01.17.426956; this version posted January 17, 2021. The copyright holder for this preprint (which was not certified by peer review) is the author/funder, who has granted bioRxiv a license to display the preprint in perpetuity. It is made available under aCC-BY-NC-ND 4.0 International license.

Regulation of bacterial Type III Secretion System export gate opening

Authors

Owain J. Bryant[a,b,*], Gillian M. Fraser[a,*]

Affiliations

[a]Department of Pathology, University of Cambridge, Tennis Court Road, Cambridge, CB2 1QP, United Kingdom

Corresponding authors

[*]Gillian M. Fraser

Department of Pathology, University of Cambridge, Tennis Court Road, Cambridge, CB2 1QP, United Kingdom

Phone: +44 1223 330245 Email: gmf29@cam.ac.uk

[*]Owain J. Bryant

Department of Pathology, University of Cambridge, Tennis Court Road, Cambridge, CB2 1QP, United Kingdom

Phone: +44 1223 366145 Email: owain.bryant@bioch.ox.ac.uk

[b]Current address: Department of Biochemistry, University of Oxford, South Parks Road, Oxford, OX1 3QU

Keywords

Type III secretion; protein export; bacterial flagella biogenesis

bioRxiv preprint doi: https://doi.org/10.1101/2021.01.17.426956; this version posted January 17, 2021. The copyright holder for this preprint (which was not certified by peer review) is the author/funder, who has granted bioRxiv a license to display the preprint in perpetuity. It is made available under aCC-BY-NC-ND 4.0 International license.

Abstract

Type III Secretion Systems (T3SS) transport proteins from the bacterial cytosol for assembly into cell surface nanomachines or for direct delivery into target eukaryotic cells. At the core of the flagellar T3SS, the FlhAB-FliPQR export gate regulates protein entry into the export channel whilst maintaining the integrity of the cell membrane. Here, we identify critical residues in the export gate FliR plug that stabilise the closed conformation, preserving the membrane permeability barrier, and we show that the gate opens and closes in response to export substrate availability. Our data indicate that FlhAB-FliPQR gate opening, which is triggered by substrate export signals, is energised by FlhA in a proton motive force-dependent manner. We present evidence that the export substrate and the FliJ stalk of the flagellar ATPase provide mechanistically distinct, non-redundant gate-activating signals that are critical for efficient export.

Introduction

Type III Secretion Systems (T3SS) transport proteins across the bacterial inner and outer membranes and, in the case of the virulence T3SS (vT3SS), across the plasma membrane of target eukaryotic cells [1,2,3]. The flagellar T3SS (fT3SS) is required for assembly of rotary flagella, which facilitate cell motility[1,2,3,4]. Despite their different functions, the vT3SS and fT3SS are evolutionarily related and contain conserved core export components[5,6,7,8,9,10,11].

For construction of the bacterial flagellum, most of the flagellar components are exported by the fT3SS machinery, which is embedded in the cell envelope. The core of the export machinery is made up of five highly conserved proteins (FlhA, FlhB, FliP, FliQ and FliR). FlhA forms a nonameric ring structure comprising a

bioRxiv preprint doi: https://doi.org/10.1101/2021.01.17.426956; this version posted January 17, 2021. The copyright holder for this preprint (which was not certified by peer review) is the author/funder, who has granted bioRxiv a license to display the preprint in perpetuity. It is made available under aCC-BY-NC-ND 4.0 International license.

cytoplasmic domain which functions as a docking platform for export cargo and an N-terminal region ($FlhA_N$) with putative proton conducting activity[5,12,13,14]. Recent cryo-ET data has shown that $FlhA_N$ wraps around the base of a helical-dome composed of FliPQR and the N-terminal region of FlhB ($FlhB_N$)[13]. Together, FlhA and $PQRB_N$ constitute the ABPQR export gate, which regulates entry of flagellar subunits into the central channel that runs the length of the nascent flagellum[5,12,13]. In addition to the ABPQR export gate, an ATPase complex (FliHIJ) located in the cytoplasm converts the fT3SS into a highly efficient pmf-driven protein export machine[10,15,16,17].

Recent structural studies of FliPQR and $FlhB_N$ have shown that multiple interactions stabilise the closed export gate [5,6,12,18]. A central plug formed by residues 106-120 of FliR, a methionine rich loop (M-gate) within FliP, and ionic interactions between adjacent FliQ subunits maintain the closed conformation[5,6,18]. Structural analysis of the export gate in the open conformation revealed multiple rearrangements within the M-gate and an upward displacement of the FliR plug, indicating that energy must be provided to open the gate and permit subunit translocation across the inner membrane[18]. We reasoned that, as the PQRB components of the gate are positioned adjacent to the proposed proton conducting FlhA membrane protein, FlhA might use the energy derived from the pmf to promote gate opening. Moreover, we hypothesised that gate opening must be regulated by one or more factors to permit subunit export whilst maintaining the membrane permeability barrier. We set out to test these hypotheses experimentally.

bioRxiv preprint doi: https://doi.org/10.1101/2021.01.17.426956; this version posted January 17, 2021. The copyright holder for this preprint (which was not certified by peer review) is the author/funder, who has granted bioRxiv a license to display the preprint in perpetuity. It is made available under aCC-BY-NC-ND 4.0 International license.

Results

Replacement of critical residues in the FliR plug destabilises the closed conformation of the fT3SS export gate.

The fT3SS ABPQR export gate resides in a closed conformation in the absence of subunit export[5,6,13,11,18]. We set out to engineer the export gate to destabilise the closed conformation and favour the open state, reasoning that mutation of contact points between adjacent gate subunits would reduce the energy barrier required for gate opening (Fig.1A). To screen for potential gate opening mutants, we used a subunit variant ($FlgD_{short}$) that we have previously shown is unable to trigger efficient opening of the export gate[19]. We predicted that mutations which promoted export gate opening would also supress the $FlgD_{short}$ motility defect. Recent structural information has revealed the potential gating mechanism of the FliPQR gate components. A region of FliR (residues 106-121) forms a plug that occludes the gate channel, and this plug must be displaced to achieve gate opening[18]. In the FliR plug, residues Phe-110 and Phe-113 make multiple contacts within the core of the export gate, and might have a central role in gate opening[5,12]. To assess the importance of selected FliR residues in gate opening, we replaced Phe-110 and/or Phe-113 with alanine, and replaced Gly-117 with a bulkier charged aspartate residue and screened for suppression of the $FlgD_{short}$ motility defect (Fig. 1). We found that all three of these FliR-plug mutations ($F_{110}A$, $F_{113}A$ and $G_{117}D$) supressed the $FlgD_{short}$ motility defect, yet did not increase export or motility of cells encoding wild type FlgD (Fig. 1B, 1C and S1, S2), indicating these mutations destabilise the closed export gate conformation. The FliR-$G_{117}D$ mutation was previously proposed to rescue an interaction between FliR and FlhA, but the data presented here indicate that the

bioRxiv preprint doi: https://doi.org/10.1101/2021.01.17.426956; this version posted January 17, 2021. The copyright holder for this preprint (which was not certified by peer review) is the author/funder, who has granted bioRxiv a license to display the preprint in perpetuity. It is made available under aCC-BY-NC-ND 4.0 International license.

74 $G_{117}D$, $F_{113}A$ and $F_{115}A$ mutations destabilise the closed conformation of the export
75 gate (Fig. 1D)[20].
76
77 We hypothesised that deletion of the FliR plug would promote the open gate
78 conformation and, as a result, increase the permeability of the inner membrane.
79 Bacterial cells that fail to maintain the permeability barrier across the inner
80 membrane are more sensitive to a number of chemical agents, such as choline[21]. To
81 determine whether a strain encoding a FliR plug deletion variant (FliRΔ110-116,
82 hereafter termed FliRΔplug) was sensitive to choline, we performed growth inhibition
83 assays by culturing cells in media containing increasing concentrations of choline
84 (Fig 1E). We found that the FliRΔplug strain was sensitised to choline compared to
85 wild type *Salmonella*, indicating that the FliR plug is important for formation of a tight
86 barrier that is impermeable to small molecules, and for maintaining the closed
87 conformation of the fT3SS export gate (Fig. 1E, 1F, S3).
88
89 **The export gate fluctuates between open and closed states in response to**
90 **substrate availability**
91 A previous study showed the $M_{210}A$ mutation in the FliP component of the export
92 gate sensitised cells to a variety of chemical agents[21]. This sensitivity could be
93 reversed by trapping a subunit in the export channel, suggesting that the export gate
94 can form an effective seal around a substrate during transit[21]. We reasoned that if
95 the export gate fluctuates between open and closed conformations in response to
96 the availability of substrate, strains producing fewer flagellar subunits would, at any
97 given time, have fewer subunits transiting through the fT3SS to seal the leaky

bioRxiv preprint doi: https://doi.org/10.1101/2021.01.17.426956; this version posted January 17, 2021. The copyright holder for this preprint (which was not certified by peer review) is the author/funder, who has granted bioRxiv a license to display the preprint in perpetuity. It is made available under aCC-BY-NC-ND 4.0 International license.

FliRΔplug gate. To test this, we constructed a strain deleted for the genes that encode most of the early flagellar subunits by replacing a large portion of the *flg* operon (*flgB*, *flgC*, *flgD*, *flgE*, *flgF*, *flgG*, *flgH*, *flgI* and *flgJ*) with a kanamycin resistance cassette. In addition, we constructed a second strain in which the FliR plug and the rod/hook genes were deleted. This FliRΔplug-Δsubunit strain was significantly more sensitive to choline than the FliRΔplug strain, indicating that actively transiting subunits partially seal the export gate when the FliR plug is absent (Fig. 1E, 1F, S3). Notably, the Δsubunit strain (which produces wild type FliR) was not more sensitive to choline than wild type *Salmonella*, indicating that decreased subunit availability does not increase the permeability of the wild type export gate to small molecules (Fig. 1E, 1F, 1G). This suggests that the export gate must fluctuate between open and tightly closed conformations, in response to availability of subunits at the export machinery.

Destabilising the closed conformation of the export gate alleviates the export defect associated with a variant of the gate component FlhA.

Opening of the export gate is thought to be energised, in part, by harnessing of the pmf by FlhA. A previous study proposed that FlhA interacts with FliR, as mutations in *fliR* were found to suppress the motility defect of a weakly motile *Salmonella* (Δ*fliH-fliI, flhB*-$P_{28}T$*, flhA*-$K_{203}W$) that contained deletions in flagellar ATPase genes (*fliI* and *fliH*), a suppressor mutation in *flhB,* $P_{28}T$, which overcomes the loss of FliH and FliI, and a mutation in *flhA,* $K_{203}W$, that attenuates motility and export [20]. However, structural studies subsequently revealed that these FliR suppressor mutations are located in the core of the FliPQR complex, indicating that this region of FliR is unable

bioRxiv preprint doi: https://doi.org/10.1101/2021.01.17.426956; this version posted January 17, 2021. The copyright holder for this preprint (which was not certified by peer review) is the author/funder, who has granted bioRxiv a license to display the preprint in perpetuity. It is made available under aCC-BY-NC-ND 4.0 International license.

to contact FlhA within the assembled fT3SS[5]. We have shown that one of these suppressor mutations in the FliR plug (FliR-$G_{117}D$) destabilises the closed conformation of the export gate (Fig. 1B and 1C). Based on these data, we hypothesised that FliR-$G_{117}D$ might suppress the motility and export defects associated with mutation of FlhA-K_{203} by destabilising the closed conformation of the export gate, rather than by restoring an interaction between FliR and FlhA. To test this, we assessed whether the export and motility of strains encoding FlhA-$K_{203}A$ could be recovered by introducing mutations (FliR-$F_{113}A$ or FliR-$G_{117}D$) that destabilise the closed gate conformation. We found that, as predicted, FliR-$F_{113}A$ and FliR-$G_{117}D$ suppressed the export and motility defects associated with FlhA $K_{203}A$ (Fig. 2). The data indicate that the *flhA*-$K_{203}A$ strain is unable to open the export gate efficiently and that introduction of *fliR* mutations that destabilise the closed gate might lower the energy barrier that must be overcome by FlhA-$K_{203}A$ to open the gate (Fig. 2A-2B).

Increasing the pmf suppresses the FlhA-$K_{203}A$ export defect

Our results support the view that FlhA has a role in opening the export gate and that FlhA-K_{203} is critical for efficient gate opening. As FlhA has been proposed to facilitate subunit export by functioning as a proton-conducting channel[14,17,20], we hypothesised that the FlhA-$K_{203}A$ mutation might render the export machinery unable to couple pmf to efficient gate opening. If this were the case, the gate opening and subunit export defects of a strain carrying chromosomally encoded *flhA-$K_{203}A$* might be overcome by increasing the pmf. To test this, we artificially increased the pmf across the bacterial inner membrane by driving intracellular proton consumption[22].

bioRxiv preprint doi: https://doi.org/10.1101/2021.01.17.426956; this version posted January 17, 2021. The copyright holder for this preprint (which was not certified by peer review) is the author/funder, who has granted bioRxiv a license to display the preprint in perpetuity. It is made available under aCC-BY-NC-ND 4.0 International license.

Cells supplemented with arginine convert intracellular protons and arginine to agmatine and CO_2 through the action of the cytoplasmic enzyme arginine decarboxylase, which effectively acts as a proton sink in the cytosol and therefore increases the pmf[22] (Fig. 3A). We performed a modified subunit export assay in which cells were grown to mid-exponential phase, washed, resuspended in media containing 20 mM arginine and culture supernatants were collected after 30 mins. Addition of arginine to cultures of the *flhA*-K_{203}A strain increased subunit export by 40%, whereas subunit export in the wild type strain was unchanged (Fig. 3B). Deletion of the two arginine decarboxylase enzymes (*speA* and *adiA*) encoded by *Salmonella* abolished the arginine-dependent increase in subunit export by the *flhA*-K_{203}A strain, indicating that the FlhA-K_{203}A mutation prevented efficient use of the pmf by the export machinery. The data are consistent with wild type FlhA utilising the pmf to energise export gate opening (Fig. S4).

Two distinct non-redundant signals activate the pmf-driven export machinery

We have found that the N-terminus of rod/hook subunits contains a hydrophobic signal that triggers opening of the export gate[19], a process that would require an input of energy from either the flagellar ATPase and/or the proton motive force. We reasoned that the subunit 'gate opening' signal must somehow be transmitted to FlhA, triggering it to energise opening of the export gate. Previous studies have shown that, in addition, interaction of FlhA with the FliJ stalk component of the ATPase is required to convert the fT3SS into a highly efficient $\Delta\psi$ driven export machine, suggesting that the FliJ-FlhA interaction might be a second signal required for export gate opening[17]. Loss of either the FliJ-FlhA interaction or the subunit N-

bioRxiv preprint doi: https://doi.org/10.1101/2021.01.17.426956; this version posted January 17, 2021. The copyright holder for this preprint (which was not certified by peer review) is the author/funder, who has granted bioRxiv a license to display the preprint in perpetuity. It is made available under aCC-BY-NC-ND 4.0 International license.

terminal hydrophobic signal can be overcome by suppressor mutations in the export machinery: FliH-FliI-FliJ loss can be overcome by mutations in FlhA or FlhB[23,24], and we have shown that loss of the interaction between the $FlgD_{short}$ subunit N-terminal hydrophobic signal and the export machinery can be overcome by mutations in the genes encoding FliP or FliR that destabilise the export gate closed conformation[19]. We now wanted to test whether the suppressor mutations in the ABPQR export gate (FliR-$F_{113}A$ or FliR-$G_{117}D$) that recovered export of $FlgD_{short}$ could also recover motility and export in strains deleted for the ATPase genes (in which the FliJ-FlhA is lost; Fig. 4A and 4B). To test this, we constructed strains in which the chromosomal *fliR* gene was replaced with *fliR* alleles containing the gate opening mutations ($F_{113}A$ or $G_{117}D$) in combination with deletions in the genes that encode the ATPase components FliH and FliI. These strains were also deleted for the gene encoding the flagellar anti-sigma factor FlgM, which is exported during the filament stage of assembly[25]. Deletion of *flgM* ensures that flagellar gene expression is not influenced by any differences in export efficiency between strains[26] (Fig. 4). Mutations that promoted the open gate conformation (FliR-$F_{113}A$ or FliR-$G_{117}D$) did not recover motility and export in strains deleted for the ATPase complex (Fig. 4A and 4B). This indicates that mutations that promote the open conformation of the FliPQR gate cannot bypass the loss of FliJ-dependent activation of FlhA.

We then assessed whether the FlhB-$P_{28}T$ suppressor, which enables bypass of flagellar ATPase activity (and, as a result, bypass of the FliJ-FlhA interaction), could recover efficient gate opening by $FlgD_{short}$ (Fig. 4C). A *Salmonella flgD* null strain encoding *flhB*-$P_{28}T$ and producing $FlgD_{short}$ was found to be no more motile than the parental *Salmonella flgD* null strain producing $FlgD_{short}$ (Fig 4C and S5).

bioRxiv preprint doi: https://doi.org/10.1101/2021.01.17.426956; this version posted January 17, 2021. The copyright holder for this preprint (which was not certified by peer review) is the author/funder, who has granted bioRxiv a license to display the preprint in perpetuity. It is made available under aCC-BY-NC-ND 4.0 International license.

194 This indicates that the FlhB-P_{28}T mutation does not promote opening of the export
195 gate, but instead restores fT3SS activity in the absence of the FliJ activation signal
196 by an alternative mechanism (Fig. 4C).

197 These data indicate that mutations in *fliP* or *fliR* that promote the open
198 conformation of the export gate and mutations that bypass the need for the FliJ-FlhA
199 interaction are unable to compensate for each other, indicating that the subunit N-
200 terminal hydrophobic export signal and the FliJ-FlhA interaction signal are non-
201 redundant, *i.e.* both signals are required to activate pmf-driven opening of the
202 ABPQR export gate by FlhA (Fig. 5).

203

204 **Discussion**

205 Transport of substances across the bacterial inner membrane is highly
206 selective, thereby maintaining the essential electrochemical gradients that drive
207 numerous processes at the cell membrane, including ATP synthesis and protein
208 export. The fT3SS translocates proteins efficiently across the inner membrane
209 without compromising the permeability barrier[5,18,21]. The ABPQR flagellar export gate
210 contains three constriction points that are proposed to maintain the gate in a closed
211 conformation, preserving the integrity of the membrane permeability barrier[5]. Here,
212 we identified point mutant and deletion variants of proteins in the ABPQR export gate
213 that destabilise its closed conformation. We show that either by destabilising the
214 export gate closed conformation or by increasing the pmf, the flagellar export defects
215 of strains encoding FlhA-K_{203}A can be alleviated, indicating that FlhA harnesses the
216 pmf to energise opening of the export gate complex. Additional *in vivo* experiments
217 revealed that FlhA requires activation by both the flagellar ATPase stalk component

bioRxiv preprint doi: https://doi.org/10.1101/2021.01.17.426956; this version posted January 17, 2021. The copyright holder for this preprint (which was not certified by peer review) is the author/funder, who has granted bioRxiv a license to display the preprint in perpetuity. It is made available under aCC-BY-NC-ND 4.0 International license.

FliJ and an N-terminal hydrophobic signal in the export substrate to trigger efficient gate opening and subunit export.

Mutational analysis of the FliR-plug identifies variants that destabilise the closed conformation of the export gate.

Structures of the FliPQR export gate have revealed that, in the absence of the export substrate, multiple non-covalent interactions in the gate complex stabilise the closed conformation[5,12,18]. In particular, a 15-residue region of FliR forms a plug that occludes the central channel of the gate. Two residues within the FliR-plug, FliR-F_{113} and FliR-F_{115}, interact with a concentric ring of conserved methionine residues (M-gate) in FliP[5]. Our mutational analyses identified FliR variants, FliR-F_{113}A and FliR-F_{115}A, that destabilise the closed conformation of the export gate[5], indicating that these residues help to maintain the gate in its closed state in the absence of export substrate. An additional FliR-plug variant, FliR-G_{117}D, also destabilised the closed gate, suggesting that the introduction of a bulky, charged side chain at this site prevents tight closure of the gate. A recent structure of the open export gate revealed multiple rearrangements within the M-gate and an upward displacement of the FliR plug to allow subunit passage[18]. This indicates that the FliR plug, which occludes the export channel in the closed gate conformation, must be displaced to allow passage of unfolded subunits through the gate. A strain containing a deletion within the FliR-plug (residues 110-116) displayed choline sensitivity, consistent with the plug forming a tight seal to maintain the membrane permeability barrier (Fig 1). Notably, we found that a FliR-plug deletion strain that produced fewer subunits was significantly more sensitive to choline than a strain that encoded wild type FliR and

bioRxiv preprint doi: https://doi.org/10.1101/2021.01.17.426956; this version posted January 17, 2021. The copyright holder for this preprint (which was not certified by peer review) is the author/funder, who has granted bioRxiv a license to display the preprint in perpetuity. It is made available under aCC-BY-NC-ND 4.0 International license.

produced fewer subunits (Fig 1). These data indicate that (i) subunit transit through the export gate can partially rescue the choline-sensitive phenotype associated with loss of the FliR-plug, and (ii) that when no subunits available for transit, the wild type export gate closes to maintain the membrane permeability barrier. These observations have important implications for our understanding of how the export gate opens. Sequential rounds of gate opening and closing must occur in response to the presence or absence of export substrates at the membrane export machinery. Similar gating mechanisms have been observed in other protein conducting channels, such as the SecY channel, which similarly contains a constriction formed by ring of hydrophobic residues and a central plug that forms a seal[27]. Deletion of either the central plug or the ring of hydrophobic residues in SecY results in increased permeability of the channel, and electrophysiology experiments showed that these deletions cause the channel to alternate between an open and closed state[28]. Furthermore, molecular dynamic simulations indicate that the force required for opening the gate is reduced in SecY plug deletion mutants[29]. We found that deletion of the FliR plug similarly destabilised the closed conformation of the export gate and concomitantly increased permeability of the inner membrane (Fig. 1).

FlhA activity is required for efficient opening of the export gate.

A previous study identified suppressor mutations in the gene encoding FliR that rescued the export defect of a strain that contained mutations in *flhA* ($K_{203}W$) and *flhB* ($P_{28}T$), as well as deletions in the genes encoding flagellar export ATPase components (*fliH* and *fliI*)[20]. The authors proposed that the FliR suppressor mutations might recover an interaction between FliR and FlhA[20]. One of these

bioRxiv preprint doi: https://doi.org/10.1101/2021.01.17.426956; this version posted January 17, 2021. The copyright holder for this preprint (which was not certified by peer review) is the author/funder, who has granted bioRxiv a license to display the preprint in perpetuity. It is made available under aCC-BY-NC-ND 4.0 International license.

suppressor mutations (FliR-$G_{117}D$) is positioned within the core of the FliPQR complex and introduces a bulky, charged side chain into the lumen of the export gate. We showed that the FliR-$G_{117}D$ mutation partially suppressed the motility defect associated with a subunit ($FlgD_{short}$) that is unable to trigger efficient opening of the export gate, indicating that the FliR-$G_{117}D$ mutation might instead destabilise the export gate's closed conformation (Fig. 1B and 1C). We hypothesised that by the same mechanism, the FliR-$G_{117}D$ mutation might also suppress the motility and export defects associated with FlhA-K_{203}. *Salmonella* strains carrying the *flhA*-$K_{203}A$ mutation in combination with mutations in *fliR* ($F_{113}A$ or $G_{117}D$), which destabilise the closed conformation of the export gate, displayed enhanced flagellar export and motility compared to the parental *Salmonella flhA*-$K_{203}A$ strain (Fig. 2). This indicates that FlhA-$K_{203}A$ is unable to facilitate efficient export gate opening and, as a result, attenuates subunit export and cell motility.

Cryo-electron tomograms of the *Salmonella* injectisome have revealed that the FlhA homologue, InvA, is positioned adjacent to the homologues of the FliPQR export gate components, SpaPQR[13]. As FlhA is proposed to function as a proton conducting channel that energises export, we reasoned proton translocation might be coupled to gate opening, possibly through transmission of conformational changes in FlhA to the adjacent FliPQR-FlhB components of the export gate[13,14,20]. In support of this view, we found that by increasing the pmf across the inner membrane, through supplementation of cell cultures with arginine, subunit export by the *flhA*-$K_{203}A$ strain could be enhanced by 40%, suggesting that inefficient export in the *flhA*-$K_{203}A$ strain is caused by its decreased ability to couple the pmf to gate opening (Fig. 3A).

bioRxiv preprint doi: https://doi.org/10.1101/2021.01.17.426956; this version posted January 17, 2021. The copyright holder for this preprint (which was not certified by peer review) is the author/funder, who has granted bioRxiv a license to display the preprint in perpetuity. It is made available under aCC-BY-NC-ND 4.0 International license.

Two distinct signals activate the pmf-driven export machinery.

Previous studies have shown that the FliJ stalk component of the flagellar ATPase interacts with FlhA to convert the export machinery into a highly efficient $\Delta\psi$-driven export machine[17,30,31,32]. The FliH and FliI components of the ATPase facilitate the FliJ-FlhA interaction to promote full activation of the export gate[17,31]. These findings indicate that FliJ binding to FlhA modulates its proton conducting ability, analogous to the interactions between the stalk component of the F_1 ATPase and the membrane-localised F_0 channel that drive proton translocation across the bacterial inner membrane. The need for activation of FlhA by the FliJ stalk, to facilitate efficient use of the $\Delta\psi$ component of the pmf and energise gate opening, can be bypassed by mutations in *flhA* and *flhB* that overcome the loss of the flagellar ATPase [8,23,24].

In addition to the FilJ-dependent gate opening signal, we have previously shown that a subunit N-terminal hydrophobic signal is required to trigger opening of the export gate[19] (Fig. 1C). To determine whether both signals were required to trigger opening of the export gate or whether the signals were functionally redundant, we asked if suppressor mutations in the ABPQR export gate (FliR-F_{113}A or FliR-G_{117}D) that could compensate for loss of the subunit N-terminal hydrophobic signal could also overcome loss of the flagellar ATPase (and of the FilJ-dependent gate opening signal). We found that neither FliR-F_{113}A nor FliR-G_{117}D could suppress the export defect caused by the loss of FliJ-dependent activation of FlhA (Fig.4). Taking the reciprocal approach, we found that a mutation in *flhB* (P_{28}T) that alleviates the loss of the FliJ-dependent activation signal could not overcome loss of the subunit N-terminal hydrophobic signal (Fig 4). This indicates that both signals are essential for

bioRxiv preprint doi: https://doi.org/10.1101/2021.01.17.426956; this version posted January 17, 2021. The copyright holder for this preprint (which was not certified by peer review) is the author/funder, who has granted bioRxiv a license to display the preprint in perpetuity. It is made available under aCC-BY-NC-ND 4.0 International license.

314 efficient opening of the flagellar export gate. We propose that FliJ binding to FlhA
315 and the presence of a subunit at the export machinery induce distinct conformational
316 changes in FlhA, rendering the export machinery competent to utilise the pmf to
317 energise opening of the export gate. The lack of either signal prevents opening of the
318 export gate and, in turn, maintains the membrane permeability barrier (Fig. 5).
319 Based on the structural and functional similarities between the core
320 components of the injectosome and flagellar Type III Secretion Systems, it is highly
321 probable that the mechanism of export gate opening is conserved. In summary, we
322 propose that the pmf induces conformational changes in FlhA that are transmitted to
323 the adjacent FliPQR-$FlhB_N$ components of the export gate, energising gate opening.
324 We demonstrate that FlhA requires at least two distinct signals to facilitate subunit
325 export: a FliJ-dependent activation signal and a subunit docked at the export
326 machinery. Our data suggest a multi-signal control system that acts *via* FlhA to
327 ensure that use of the pmf and export gate opening only occurs when a FliJ
328 activation signal is received and a subunit is available for export.
329

330 **Materials and Methods**

331 ***Bacterial strains, plasmids and growth conditions***

332 *Salmonella* strains and plasmids used in this study are listed in table 1. The
333 Δ*flgD*::K_m^R strain in which the *flgD* gene was replaced by a kanamycin resistance
334 cassette and the Δ*flgBCDEFGHIJ*::Km^R strain in which a large portion of the *flg*
335 operon was replaced with a kanamycin cassette were constructed using the λ Red
336 recombinase system[33,34]. Strains containing chromosomally encoded FliR and/or
337 FlhA variants were constructed by aph-I-SceI Kanamycin resistance cassette

bioRxiv preprint doi: https://doi.org/10.1101/2021.01.17.426956; this version posted January 17, 2021. The copyright holder for this preprint (which was not certified by peer review) is the author/funder, who has granted bioRxiv a license to display the preprint in perpetuity. It is made available under aCC-BY-NC-ND 4.0 International license.

replacement using pWRG730[34]. Recombinant proteins were expressed in *Salmonella* from isopropyl β-D-thiogalactoside-inducible (IPTG) inducible plasmid pTrc99a[35]. Bacteria were cultured at 30–37 °C in Luria-Bertani (LB) broth containing ampicillin (100 µg/ml).

Choline sensitivity assay

The choline sensitivity assay was performed essentially as described in Ward *et al.*[21]. Cells were grown overnight at 32°C in terrific broth (TB) medium with shaking (200 PRM). The overnight cultures were diluted 1:50 in TB and grown at 32°C with shaking (200 RPM) to an A600 1.0. These cultures were diluted 1:50 in TB containing choline at concentrations as indicated in Figure 2. The cultures were grown for 4.5 hours at 32°C with shaking (200 RPM) and the A_{600} measured. The Miles and Misra method[36] was used to determine the colony forming units for strains grown in 300 mM choline. 10-fold dilutions of culture were spotted (10 µl) onto LB agar plates and grown overnight at 37°C.

Flagellar subunit export assay

Salmonella strains were cultured at 37 °C in LB broth containing ampicillin and IPTG to mid-log phase (OD_{600nm} 0.6-0.8). Cells were centrifuged (6000*g*, 3 min) and resuspended in fresh media and grown for a further 60 minutes at 37 °C. Cells were pelleted by centrifugation (16,000*g*, 5 min) and the supernatant passed through a 0.2 µm nitrocellulose filter. Proteins were precipitated with 10% trichloroacetic acid (TCA) and 1% Triton-X100 on ice for 1 hour, pelleted by centrifugation (16,000*g*, 10 min), washed with ice-cold acetone and resuspended in SDS-PAGE loading buffer

bioRxiv preprint doi: https://doi.org/10.1101/2021.01.17.426956; this version posted January 17, 2021. The copyright holder for this preprint (which was not certified by peer review) is the author/funder, who has granted bioRxiv a license to display the preprint in perpetuity. It is made available under aCC-BY-NC-ND 4.0 International license.

(volumes calibrated according to cell densities). Fractions were analysed by immunoblotting. For the export assays of strains supplemented with arginine, cells were treated essentially as described above except cells were resuspended in fresh media supplemented with 20 mM arginine and grown for a further 30 minutes instead of 60 minutes.

Motility assays

For swimming motility, cultures were grown in LB broth to A600nm 1. Two microliters of culture were inoculated into soft tryptone agar (0.3% agar, 10 g/L tryptone, 5g/L NaCl) containing ampicillin (100 µg/ml). Plates were incubated at 37 °C for between 4 and 6 hours unless otherwise stated. For swarming motility, one microliter of overnight culture grown in LB broth was inoculated onto tryptone agar plates (0.6% agar, 1% w/v tryptone, 0.5% w/v sodium chloride) containing appropriate antibiotics and inducing agents and supplemented with 0.3% glucose and incubated at 30 °C for 12-16 hours.

Screen for motile suppressors from the flhA-K_{203}A variant

Cells of the *Salmonella flhA*-K_{203}A *strain* were cultured at 37 °C in LB broth to mid-log phase and inoculated into soft tryptone agar (0.3% agar, 10 g/L tryptone, 5g/L NaCl). Plates were incubated at 30 °C until motile 'spurs' appeared. Cells from the spurs were streaked to single colony and the *flhA* gene sequenced. New strains containing the *flhA*-K_{203}A and suppressor mutations were constructed by aph-I-SceI λ Red recombination to confirm that the mutations within *flhA* were responsible for the motility suppressor phenotype[34].

bioRxiv preprint doi: https://doi.org/10.1101/2021.01.17.426956; this version posted January 17, 2021. The copyright holder for this preprint (which was not certified by peer review) is the author/funder, who has granted bioRxiv a license to display the preprint in perpetuity. It is made available under aCC-BY-NC-ND 4.0 International license.

Quantification and statistical analysis

Experiments were performed at least three times. Immunoblot were quantified using Image Studio Lite. The unpaired two-tailed Student's *t*-test was used to determine *p*-values and significance was determined as $*p < 0.05$. Data are represented as mean ± standard error of the mean (SEM), unless otherwise specified and reported as biological replicates.

Author contributions

O.J.B and G.M.F conceived and designed experiments. O.J.B conducted experiments. O.J.B analysed the data. O.J.B and G.M.F wrote the paper

Competing interests

The authors declare no competing interests.

Acknowledgements

This work was funded by a grant from the Biotechnology and Biological Sciences Research Council (BB/M007197/1) to G.M.F, and a University of Cambridge John Lucas Walker studentship to O.J.B.

Materials & Correspondence

Materials are available from the corresponding authors upon request.

bioRxiv preprint doi: https://doi.org/10.1101/2021.01.17.426956; this version posted January 17, 2021. The copyright holder for this preprint (which was not certified by peer review) is the author/funder, who has granted bioRxiv a license to display the preprint in perpetuity. It is made available under aCC-BY-NC-ND 4.0 International license.

References

1. Deng, W. *et al.* Assembly, structure, function and regulation of type III secretion systems. *Nature Reviews Microbiology* (2017). doi:10.1038/nrmicro.2017.20

2. Galán, J. E., Lara-Tejero, M., Marlovits, T. C. & Wagner, S. Bacterial Type III Secretion Systems: Specialized Nanomachines for Protein Delivery into Target Cells. *Annu. Rev. Microbiol.* (2014). doi:10.1146/annurev-micro-092412-155725

3. Evans, L. D. B., Hughes, C. & Fraser, G. M. Building a flagellum outside the bacterial cell. *Trends in Microbiology* (2014). doi:10.1016/j.tim.2014.05.009

4. Evans, L. D. B., Hughes, C. & Fraser, G. M. Building a flagellum in biological outer space. *Microb. cell (Graz, Austria)* (2014).

5. Kuhlen, L. *et al.* Structure of the core of the type iii secretion system export apparatus. *Nat. Struct. Mol. Biol.* (2018). doi:10.1038/s41594-018-0086-9

6. Johnson, S., Kuhlen, L., Deme, J. C., Abrusci, P. & Lea, S. M. The Structure of an Injectisome Export Gate Demonstrates Conservation of Architecture in the Core Export Gate between Flagellar and Virulence Type III Secretion Systems. *MBio* (2019). doi:10.1128/mbio.00818-19

7. Abrusci, P. *et al.* Architecture of the major component of the type III secretion system export apparatus. *Nat. Struct. Mol. Biol.* **20**, 99–104 (2012).

8. Saijo-Hamano, Y. *et al.* Structure of the cytoplasmic domain of FlhA and implication for flagellar type III protein export. *Mol. Microbiol.* **76**, 260–268 (2010).

bioRxiv preprint doi: https://doi.org/10.1101/2021.01.17.426956; this version posted January 17, 2021. The copyright holder for this preprint (which was not certified by peer review) is the author/funder, who has granted bioRxiv a license to display the preprint in perpetuity. It is made available under aCC-BY-NC-ND 4.0 International license.

9. Zarivach, R., Vuckovic, M., Deng, W., Finlay, B. B. & Strynadka, N. C. J. Structural analysis of a prototypical ATPase from the type III secretion system. *Nat. Struct. Mol. Biol.* **14**, 131–137 (2007).

10. Imada, K., Minamino, T., Tahara, A. & Namba, K. Structural similarity between the flagellar type III ATPase FliI and F1-ATPase subunits. *Proc. Natl. Acad. Sci. U. S. A.* **104**, 485–90 (2007).

11. Hu, J. *et al.* T3S injectisome needle complex structures in four distinct states reveal the basis of membrane coupling and assembly. *Nat. Microbiol.* (2019). doi:10.1038/s41564-019-0545-z

12. Kuhlen, L. *et al.* The substrate specificity switch FlhB assembles onto the export gate to regulate type three secretion. *Nat. Commun.* (2020). doi:10.1038/s41467-020-15071-9

13. Butan, C., Lara-Tejero, M., Li, W., Liu, J. & Galán, J. E. High-resolution view of the type III secretion export apparatus in situ reveals membrane remodeling and a secretion pathway. *Proc. Natl. Acad. Sci. U. S. A.* (2019). doi:10.1073/pnas.1916331116

14. Erhardt, M. *et al.* Mechanism of type-III protein secretion: Regulation of FlhA conformation by a functionally critical charged-residue cluster. *Mol. Microbiol.* (2017). doi:10.1111/mmi.13623

15. Ibuki, T. *et al.* Common architecture of the flagellar type III protein export apparatus and F- and V-type ATPases. *Nat. Struct. Mol. Biol.* **18**, 277–282 (2011).

16. Kishikawa, J. ichi *et al.* Common Evolutionary Origin for the Rotor Domain of Rotary Atpases and Flagellar Protein Export Apparatus. *PLoS One* **8**, (2013).

bioRxiv preprint doi: https://doi.org/10.1101/2021.01.17.426956; this version posted January 17, 2021. The copyright holder for this preprint (which was not certified by peer review) is the author/funder, who has granted bioRxiv a license to display the preprint in perpetuity. It is made available under aCC-BY-NC-ND 4.0 International license.

458 17. Minamino, T., Morimoto, Y. V., Hara, N. & Namba, K. An energy transduction
459 mechanism used in bacterial flagellar type III protein export. *Nat. Commun.*
460 (2011). doi:10.1038/ncomms1488
461 18. Sean Miletic, Dirk Fahrenkamp, Nikolaus Goessweiner-Mohr, Jiri Wald,
462 Maurice Pantel, Oliver Vesper, Vadim Kotov, and T. C. M. Substrate-engaged
463 type III secretion system structures reveal gating mechanism for unfolded
464 protein translocation. *bioRxiv* (2020).
465 19. Owain J. Bryant, Paraminder Dhillon, Colin Hughes, G. M. F. Sequential
466 recognition of discrete export signals in flagellar subunits during bacterial Type
467 III secretion. *bioRxiv* (2020).
468 20. Hara, N., Namba, K. & Minamino, T. Genetic characterization of conserved
469 charged residues in the bacterial flagellar type III export protein FlhA. *PLoS*
470 *One* **6**, (2011).
471 21. Ward, E. *et al.* Type-III secretion pore formed by flagellar protein FliP. *Mol.*
472 *Microbiol.* (2018). doi:10.1111/mmi.13870
473 22. Armbruster, C. E., Hodges, S. A., Smith, S. N., Alteri, C. J. & Mobley, H. L. T.
474 Arginine promotes Proteus mirabilis motility and fitness by contributing to
475 conservation of the proton gradient and proton motive force. *Microbiologyopen*
476 (2014). doi:10.1002/mbo3.194
477 23. Minamino, T., González-Pedrajo, B., Kihara, M., Namba, K. & Macnab, R. M.
478 The ATPase FliI can interact with the type III flagellar protein export apparatus
479 in the absence of its regulator, FliH. *J. Bacteriol.* (2003).
480 doi:10.1128/JB.185.13.3983-3988.2003
481 24. Minamino, T. & Namba, K. Distinct roles of the FliI ATPase and proton motive

bioRxiv preprint doi: https://doi.org/10.1101/2021.01.17.426956; this version posted January 17, 2021. The copyright holder for this preprint (which was not certified by peer review) is the author/funder, who has granted bioRxiv a license to display the preprint in perpetuity. It is made available under aCC-BY-NC-ND 4.0 International license.

force in bacterial flagellar protein export. *Nature* (2008). doi:10.1038/nature06449

25. Hughes, K. T., Gillen, K. L., Semon, M. J. & Karlinsey, J. E. Sensing structural intermediates in bacterial flagellar assembly by export of a negative regulator. *Science (80-.).* (1993). doi:10.1126/science.8235660

26. Chilcott, G. S. & Hughes, K. T. Coupling of Flagellar Gene Expression to Flagellar Assembly in Salmonella enterica Serovar Typhimurium andEscherichia coli. *Microbiol. Mol. Biol. Rev.* (2000). doi:10.1128/mmbr.64.4.694-708.2000

27. Van Den Berg, B. *et al.* X-ray structure of a protein-conducting channel. *Nature* (2004). doi:10.1038/nature02218

28. Saparov, S. M. *et al.* Determining the Conductance of the SecY Protein Translocation Channel for Small Molecules. *Mol. Cell* (2007). doi:10.1016/j.molcel.2007.03.022

29. Gumbart, J. & Schulten, K. The roles of pore ring and plug in the secY protein-conducting channel. *J. Gen. Physiol.* (2008). doi:10.1085/jgp.200810062

30. Minamino, T., Morimoto, Y. V., Hara, N., Aldridge, P. D. & Namba, K. The Bacterial Flagellar Type III Export Gate Complex Is a Dual Fuel Engine That Can Use Both H+ and Na+ for Flagellar Protein Export. *PLoS Pathog.* (2016). doi:10.1371/journal.ppat.1005495

31. Minamino, T. *et al.* FliH and FliI ensure efficient energy coupling of flagellar type III protein export in Salmonella. *Microbiologyopen* (2016). doi:10.1002/mbo3.340

32. Owain J. Bryant, Betty Y-W. Chung, G. M. F. Chaperone mediated coupling of

bioRxiv preprint doi: https://doi.org/10.1101/2021.01.17.426956; this version posted January 17, 2021. The copyright holder for this preprint (which was not certified by peer review) is the author/funder, who has granted bioRxiv a license to display the preprint in perpetuity. It is made available under aCC-BY-NC-ND 4.0 International license.

506 subunit availability to activation of flagellar Type III Secretion. *bioRxiv*

507 33. Datsenko, K. A. & Wanner, B. L. One-step inactivation of chromosomal genes
508 in Escherichia coli K-12 using PCR products. *Proc. Natl. Acad. Sci. U. S. A.*
509 (2000). doi:10.1073/pnas.120163297

510 34. Hoffmann, S., Schmidt, C., Walter, S., Bender, J. K. & Gerlach, R. G. Scarless
511 deletion of up to seven methylaccepting chemotaxis genes with an optimized
512 method highlights key function of CheM in Salmonella Typhimurium. *PLoS*
513 *One* (2017). doi:10.1371/journal.pone.0172630

514 35. Amann, E., Ochs, B. & Abel, K. J. Tightly regulated tac promoter vectors useful
515 for the expression of unfused and fused proteins in Escherichia coli. *Gene*
516 (1988). doi:10.1016/0378-1119(88)90440-4

517 36. Miles, A. A., Misra, S. S. & Irwin, J. O. The estimation of the bactericidal power
518 of the blood. *J. Hyg. (Lond).* (1938). doi:10.1017/S002217240001158X

519

520

bioRxiv preprint doi: https://doi.org/10.1101/2021.01.17.426956; this version posted January 17, 2021. The copyright holder for this preprint (which was not certified by peer review) is the author/funder, who has granted bioRxiv a license to display the preprint in perpetuity. It is made available under aCC-BY-NC-ND 4.0 International license.

Figure legends

Figure 1 Mutations within the FliR plug destabilise the closed export gate conformation

a. Top view of the cryo-EM structure of the closed conformation of the FliPQR export gate complex (PDB:6F2D). Phenylalanine residues 110 and 113 of FliR (grey) are displayed in red. Methionine residue 210 of FliP (blue) is displayed in magneta. FliQ is displayed in orange.

b. Swimming motility of recombinant *Salmonella flgD* null strains producing chromosomally-encoded FliR variants ($F_{110}A$, $F_{113}A$, $F_{110}A+F_{113}A$ or $G_{117}D$) or wild type FliR (FliR). Strains produced a pTrc99a plasmid-encoded FlgD subunit variant in which residues 9-32 were replaced with two repeats of the six amino acid sequence Gly-Ser-Thr-Asn-Ala-Ser ($FlgD_{short}$). Motility was assessed in 0.25% soft-tryptone agar containing 100 µg/ml ampicillin and 50 µM IPTG and incubated at 37ºC for 16 hours.

c. The mean motility halo diameter of recombinant *Salmonella flgD* null strains producing chromosomally-encoded FliR variants ($F_{110}A$, $F_{113}A$, $F_{110}A+F_{113}A$ or $G_{117}D$) or wild type FliR (FliR) and expressing the $FlgD_{short}$ variant was plotted as a percentage of the wild type FliR strain (FliR) producing $FlgD_{short}$ (right hand bar). Error bars represent the standard error of the mean calculated from at three biological replicates. * indicates a p-value < 0.05.

d. A cartoon schematic illustrating the effect of FliR plug mutations (red) on the conformation of the export gate complex (blue). Data indicates that FliR plug mutations destabilise the closed export gate conformation (left) and bias the open conformation (right).

bioRxiv preprint doi: https://doi.org/10.1101/2021.01.17.426956; this version posted January 17, 2021. The copyright holder for this preprint (which was not certified by peer review) is the author/funder, who has granted bioRxiv a license to display the preprint in perpetuity. It is made available under aCC-BY-NC-ND 4.0 International license.

e. Choline sensitivity of a *Salmonella* strain producing a chromosomally-encoded FliR variant in which residues 110-116 of the FliR plug is deleted (Δplug, grey), a *Salmonella* strain deleted for the genes (*flgBCDEFGHIJ*) that encode most of the early flagellar rod and hook subunits (Δsubunits, orange), a *Salmonella* strain that both produces the chromosomally-encoded FliRΔplug variant and is deleted for the genes (*flgBCDEFGHIJ*) that encode most of the early flagellar rod and hook subunits (ΔplugΔsubunits, blue) or a wild type *Salmonella* strain (FliR, yellow). Cells were grown in Terrific broth containing varying concentrations of choline (as indicated) and the optical density (A_{600}) measured following 4.5 hours.

f. Serial dilutions of the above *Salmonella* strains following 4.5 hours of growth in Terrific broth supplemented with 300 mM choline were spotted onto LB agar plates using the Miles and Misra method. The strains are indicated on the left and the density of the inoculum is indicated along the top.

g. A cartoon schematic illustrating the effect of the FliR plug deletion on the gating activity of the export gate complex (blue). Strains that produce fewer subunits (Δsubunits and ΔplugΔsubunits) have fewer available subunits (red) for export to seal the leaky phenotype of the export gate containing the FliR plug deletion (Δplug, right).

Figure 2 Mutations in the FliR plug suppress the FlhA-K_{203}A motility and export defects

a. Whole cell (cell) and supernatant (secreted) proteins from late exponential-phase cultures of a wild type Salmonella strain (wild type), a *Salmonella* strain producing a

bioRxiv preprint doi: https://doi.org/10.1101/2021.01.17.426956; this version posted January 17, 2021. The copyright holder for this preprint (which was not certified by peer review) is the author/funder, who has granted bioRxiv a license to display the preprint in perpetuity. It is made available under aCC-BY-NC-ND 4.0 International license.

chromosomally-encoded FlhA-$K_{203}A$ variant (FlhA $K_{203}A$) or *Salmonella* strains producing both a chromosomally-encoded FlhA-$K_{203}A$ variant and chromosomally encoded FliR variants ($F_{113}A$ or $G_{117}D$). Proteins were separated by SDS (15%)-PAGE and analysed by immunoblotting with anti-FliC, anti-FliD, anti-FlgK, anti-FlgD, anti-FlhA or anti-FlgN polyclonal antisera. Apparent molecular weights are in kilodaltons (kDa).

b. Swimming motility (0.25% soft tryptone agar) of the same strains were carried out at 37ºC for 4-6 hours.

c. Levels of FlgK in culture supernatants from Immunoblots were quantified using ImageStudiolite and plotted as a percentage of FlgK exported by the wild type strain. Error bars represent the standard error of the mean calculated from three biological replicates. * indicates a *p*-value < 0.05.

Figure 3 Increasing the proton-motive force suppresses the *flhA*-$K_{203}A$ export defect

a. A cartoon schematic of a cell containing arginine decarboxylase enzyme which catalyses the conversion of L-arginine into agmatine and carbon dioxide (CO_2). The arginine decarboxylation reaction consumes a proton (H^+) from the cell cytoplasm, reducing the number of protons in the cell, effectively increasing the proton-motive force.

b. Whole cell (cell) and supernatant (secreted) proteins from late exponential-phase cultures of a wild type *Salmonella* strain (FlhA) or a *Salmonella* strain producing a chromosomally-encoded FlhA-$K_{203}A$ variant ($K_{203}A$). Cells were supplemented with (+) or not supplemented with (-) 20 mM arginine 30 minutes prior to collection of

bioRxiv preprint doi: https://doi.org/10.1101/2021.01.17.426956; this version posted January 17, 2021. The copyright holder for this preprint (which was not certified by peer review) is the author/funder, who has granted bioRxiv a license to display the preprint in perpetuity. It is made available under aCC-BY-NC-ND 4.0 International license.

whole cell and culture supernatants. Proteins were separated by SDS (15%)-PAGE and analysed by immunoblotting with anti-FlgK, anti-FlgD, anti-FlhA or anti-FlgN polyclonal antisera (Left). Apparent molecular weights are in kilodaltons (kDa). Levels of FlgK in culture supernatants from Immunoblots for the FlhA-K_{203}A strain were quantified using ImageStudioLite and plotted as a percentage of FlgK exported by strains supplemented with arginine (+) to strains not supplemented with arginine (-) (right). Error bars represent the standard error of the mean calculated from three biological replicates. * indicates a *p*-value < 0.05.

Figure 4 Mutations in the FliR plug do not suppress export and motility defects of strains deleted for the ATPase complex

a. Swimming motility of recombinant *Salmonella* strains deleted for the genes that encode; the anti-sigma(28) factor (*flgM*), the flagellar ATPase negative regulator (*fliH*) and the flagellar ATPase subunit (*fliI*) and producing either a chromosomally-encoded FlhB-P_{28}T variant or producing chromosomally encoded wild type FliR (-) or its variants (F_{113}A or G_{117}D). Motility was assessed in 0.25% soft-tryptone agar and incubated at 37ºC for 4-6 hours.

b. Whole cell (cell) and supernatant (secreted) proteins from late exponential-phase cultures of the same strains were separated by SDS (15%)-PAGE and analysed by immunoblotting with anti-FliD, anti-FlgD, anti-FlhA or anti-FlgN polyclonal antisera. Apparent molecular weights are in kilodaltons (kDa).

c. Swimming motility of recombinant *Salmonella flgD* null strains producing chromosomally-encoded wild type FlhB or its variants (FlhB-P_{28}T). Both strains produced a pTrc99a plasmid-encoded FlgD subunit variant in which residues 9-32

bioRxiv preprint doi: https://doi.org/10.1101/2021.01.17.426956; this version posted January 17, 2021. The copyright holder for this preprint (which was not certified by peer review) is the author/funder, who has granted bioRxiv a license to display the preprint in perpetuity. It is made available under aCC-BY-NC-ND 4.0 International license.

were replaced with two repeats of the six amino acid sequence Gly-Ser-Thr-Asn-Ala-Ser ($FlgD_{short}$). Motility was assessed in 0.25% soft-tryptone agar containing 100 µg/ml ampicillin and 50 µM IPTG and incubated at 37ºC for 16 hours.

Figure 6 Two mutually exclusive signals are required to activate the export machinery and trigger opening of the export gate.

A cartoon schematic illustrating the effect of either (i) the absence of a subunits docked at the export machinery (middle, Δsubunit) or (ii) the absence of a FliJ-FlhA interaction (right, ΔFliJ) (required to convert the export machinery into a highly efficient Δψ-driven export machine) on the ability of the export machinery to energise export gate opening (blue). ATP hydrolysis by the FliI (orange, PDB: 2DPY) component of the ATPase complex is thought to drive rotation of the FliJ stalk subunit (orange, PDB: 3AJW), allowing FliJ to bind all nine binding sites on the nonameric ring of FlhA (green, PDB: 3A5I), converting the export machinery into a highly efficient Δψ-driven export machine. Early flagellar subunits dock at FlhBc (red, PDB: 3B0Z) and contain a N-terminal hydrophobic export signal required for efficient subunit export and translocation through the export gate complex (left). The absence of subunits at the export machinery (middle) or the absence of FliJ-FlhA interactions (right) renders the export machinery unable to utilise the PMF to drive opening of the export gate.

bioRxiv preprint doi: https://doi.org/10.1101/2021.01.17.426956; this version posted January 17, 2021. The copyright holder for this preprint (which was not certified by peer review) is the author/funder, who has granted bioRxiv a license to display the preprint in perpetuity. It is made available under aCC-BY-NC-ND 4.0 International license.

641 **Supplementary Figures**

642 **Figure S1**

643 Whole cell (cell) proteins from late exponential-phase cultures of recombinant
644 *Salmonella flgD* null strains producing chromosomally-encoded FliR variants ($F_{110}A$,
645 $F_{113}A$, $F_{110}A+F_{113}A$ or $G_{117}D$) or wild type FliR (FliR), and a pTrc99a plasmid-
646 encoded FlgD subunit variant in which residues 9-32 were replaced with two repeats
647 of the six amino acid sequence Gly-Ser-Thr-Asn-Ala-Ser ($FlgD_{short}$). Proteins were
648 separated by SDS (15%)-PAGE and analysed by immunoblotting with anti-FlgD
649 polyclonal antisera. Apparent molecular weights are in kilodaltons (kDa).

650

651 **Figure S2**

652 **A**. Swimming (top panel; 0.25% soft tryptone agar) and swarming (bottom panels;
653 0.6% agar-tryptone with 0.5% glucose) motility of recombinant *Salmonella* strains
654 producing chromosomally-encoded FliR variants ($F_{110}A$, $F_{113}A$, $G_{117}D$ or
655 $F_{110}A+F_{113}A$) or SJW1103 wild type.

656 **B**. Whole cell (cell) and secreted (secreted) proteins from late exponential-phase
657 cultures of recombinant *Salmonella* strains producing chromosomally-encoded FliR
658 variants ($F_{110}A$, $F_{113}A$, $G_{117}D$ or $F_{110}A+F_{113}A$) or SJW1103 wild type. Proteins were
659 separated by SDS (15%)-PAGE and analysed by immunoblotting with anti-FliC, anti-
660 FliD, anti-FlgK, anti-FlgD, anti-FlhA and anti-FlgN polyclonal antisera. Apparent
661 molecular weights are in kilodaltons (kDa).

662

663

bioRxiv preprint doi: https://doi.org/10.1101/2021.01.17.426956; this version posted January 17, 2021. The copyright holder for this preprint (which was not certified by peer review) is the author/funder, who has granted bioRxiv a license to display the preprint in perpetuity. It is made available under aCC-BY-NC-ND 4.0 International license.

664 **Figure S3**

665 Whole cell (cell) proteins from late exponential-phase cultures of recombinant
666 *Salmonella* strains producing a chromosomally-encoded FliR variant in which
667 residues 110-116 of the FliR plug is deleted (Δplug), a *Salmonella* strain deleted for
668 the genes (*flgBCDEFGHIJ*) that encode most of the early flagellar rod and hook
669 subunits (Δsubunits), a *Salmonella* strain that both produces the chromosomally-
670 encoded FliRΔplug variant and is deleted for the genes (*flgBCDEFGHIJ*) that encode
671 most of the early flagellar rod and hook subunits (ΔplugΔsubunits) and a SJW1103
672 wild type strain (FliR) were separated by SDS (15%)-PAGE and analysed by
673 immunoblotting with anti-FlhA and anti-FlgD polyclonal antisera. Apparent molecular
674 weights are in kilodaltons (kDa).

675

676 **Figure S4**

677 Whole cell (cell) and supernatant (secreted) proteins from late exponential-phase
678 cultures of a strain deleted for two genes that encode arginine decarboxylase
679 enzymes (Δ*speA* and Δ*adiA*, labelled FlhA) or a *Salmonella* Δ*speA*-Δ*adiA* strain
680 producing a chromosomally-encoded FlhA-K_{203}A variant (K_{203}A). Cells were
681 supplemented with (+) or not supplemented with (-) 20 mM arginine 30 minutes prior
682 to collection of whole cell and culture supernatants. Proteins were separated by SDS
683 (15%)-PAGE and analysed by immunoblotting with anti-FlgK, anti-FlgD, anti-FlhA or
684 anti-FlgN polyclonal antisera. Apparent molecular weights are in kilodaltons (kDa).

685

686

687

bioRxiv preprint doi: https://doi.org/10.1101/2021.01.17.426956; this version posted January 17, 2021. The copyright holder for this preprint (which was not certified by peer review) is the author/funder, who has granted bioRxiv a license to display the preprint in perpetuity. It is made available under aCC-BY-NC-ND 4.0 International license.

688 **Figure S5**

689 Whole cell (cell) proteins from late exponential-phase cultures of recombinant
690 *Salmonella flgD* null strains producing chromosomally-encoded wild type FlhB or its
691 variants (FlhB-P_{28}T). Both strains produced a pTrc99a plasmid-encoded FlgD
692 subunit variant in which residues 9-32 were replaced with two repeats of the six
693 amino acid sequence Gly-Ser-Thr-Asn-Ala-Ser ($FlgD_{short}$). Proteins were separated
694 by SDS (15%)-PAGE and analysed by immunoblotting with anti-FlgD polyclonal
695 antisera. Apparent molecular weights are in kilodaltons (kDa).

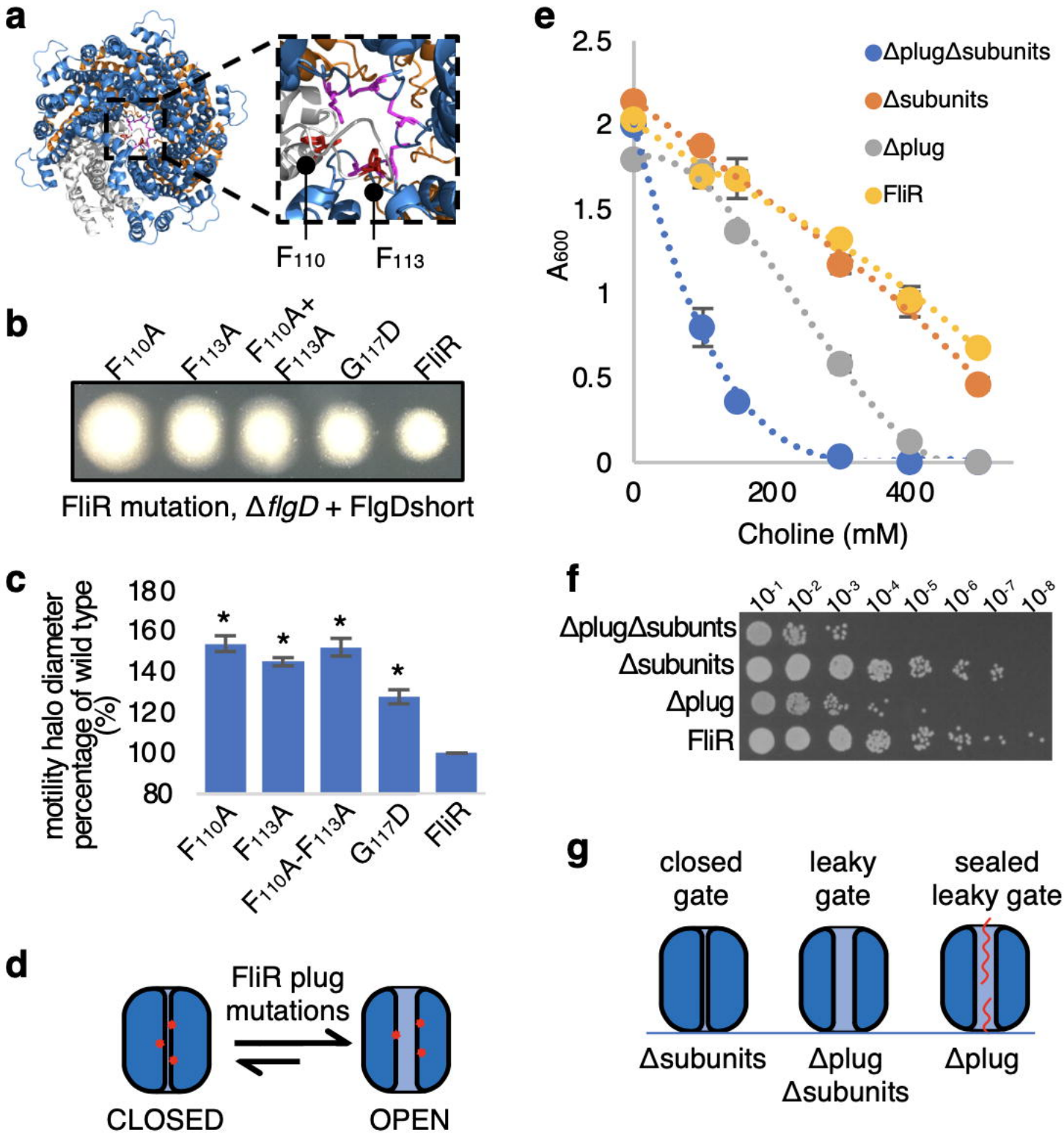
a
F110
F113
b
F110A
F113A
F110A+ F113A
G117D
FliR
FliR mutation, ΔflgD + FlgDshort
c
motility halo diameter percentage of wild type (%)
180
160
140
120
100
80
F110A
F113A
F110A-F113A
G117D
FliR
d
FliR plug mutations
CLOSED
OPEN
e
2.5
2
1.5
1
0.5
0
A600
0
200
400
Choline (mM)
ΔplugΔsubunits
Δsubunits
Δplug
FliR
f
10-1
10-2
10-3
10-4
10-5
10-6
10-7
10-8
ΔplugΔsubunts
Δsubunits
Δplug
FliR
g
closed gate
leaky gate
sealed leaky gate
Δsubunits
Δplug Δsubunits
Δplug

Figure 1

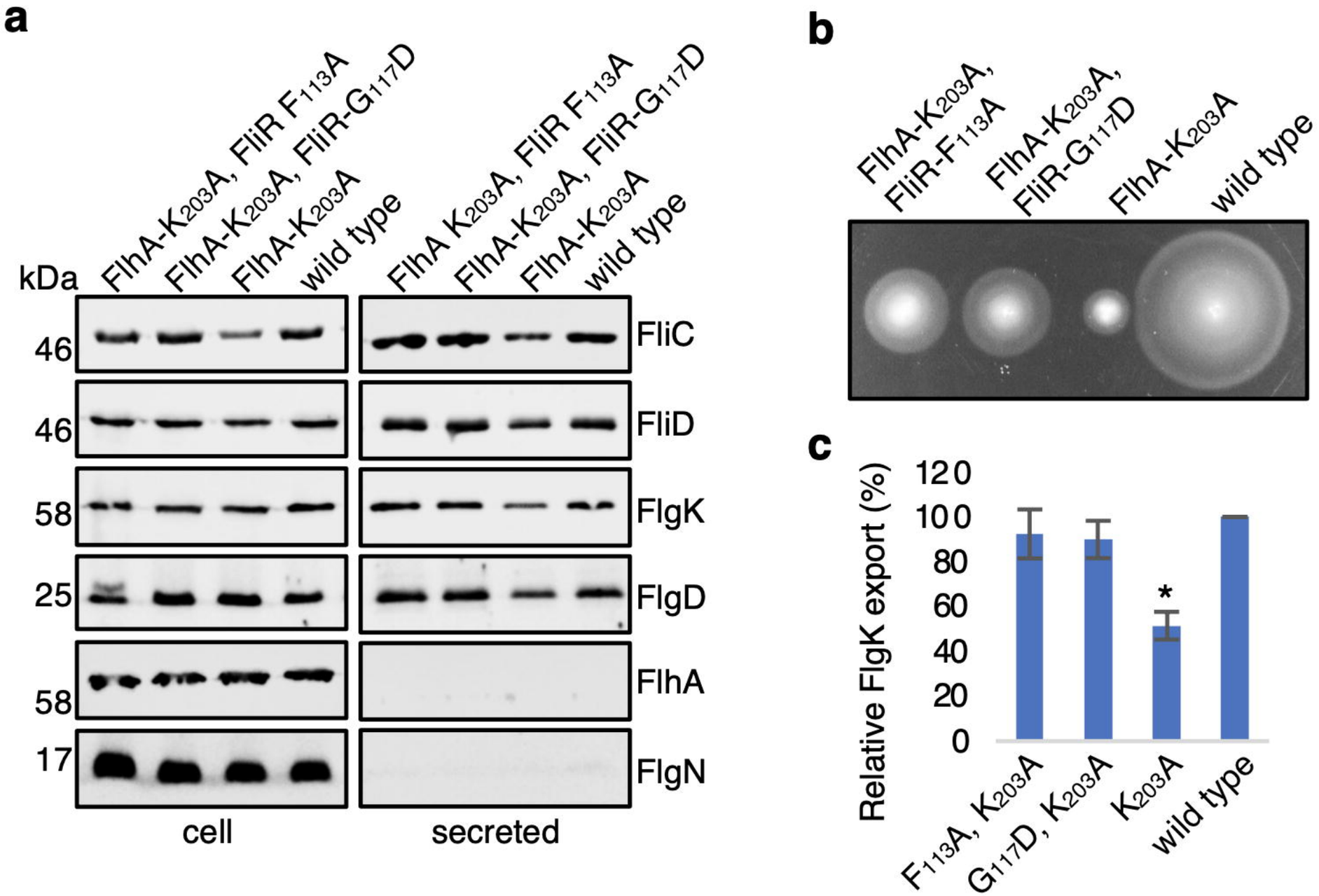
a
FlhA-K203A, FliR F113A
FlhA-K203A, FliR-G117D
FlhA-K203A
wild type
FlhA K203A, FliR F113A
FlhA-K203A, FliR-G117D
FlhA-K203A
wild type
kDa
46
46
58
25
58
17
FliC
FliD
FlgK
FlgD
FlhA
FlgN
cell
secreted
b
FlhA-K203A, FliR-F113A
FlhA-K203A, FliR-G117D
FlhA-K203A
wild type
c
Relative FlgK export (%)
120
100
80
60
40
20
0
*
F113A, K203A
G117D, K203A
K203A
wild type

Figure 2

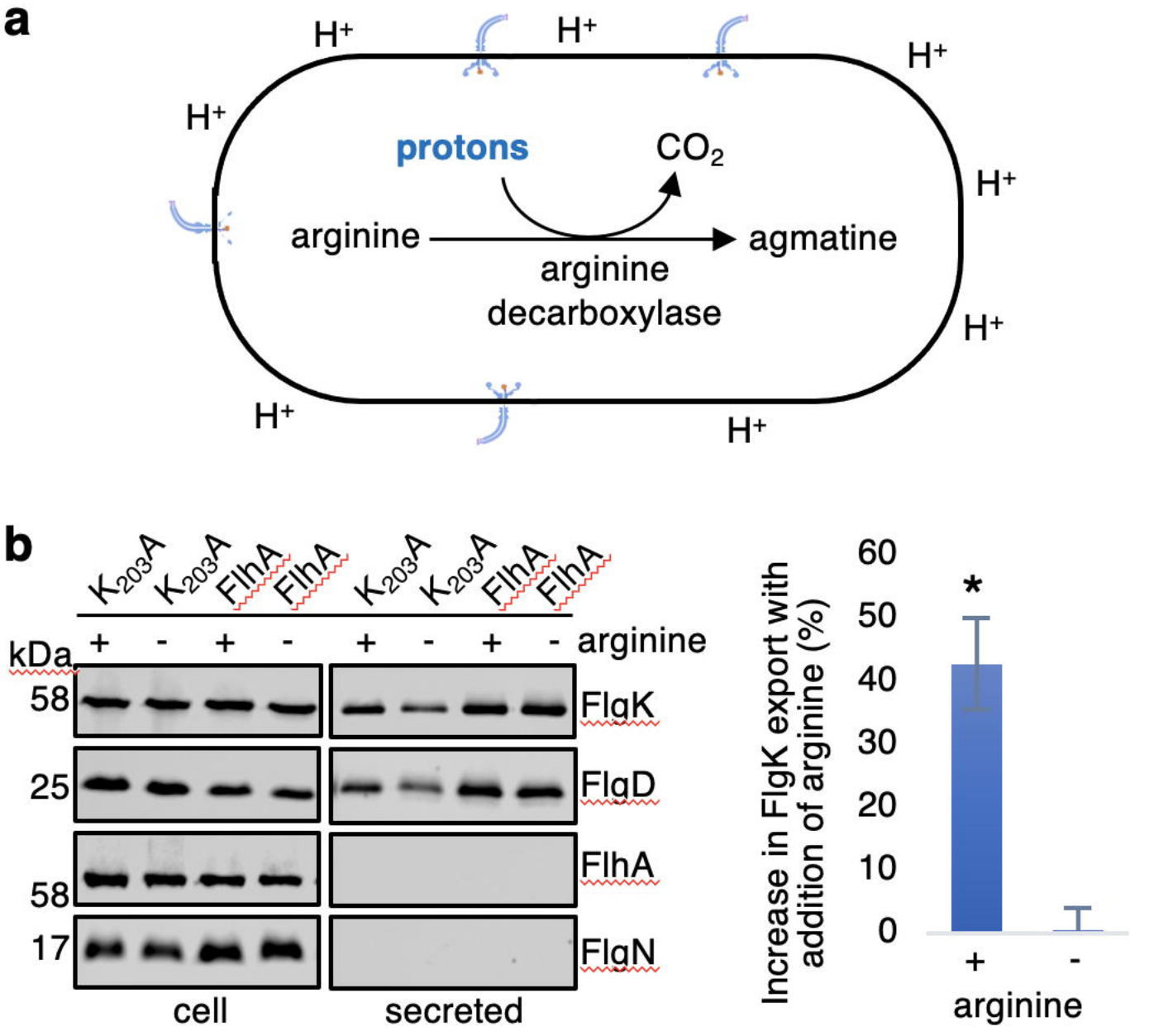
a
H+
protons
CO2
arginine
agmatine
arginine
decarboxylase
b
K203A
FlhA
kDa
+
-
arginine
58
25
58
17
FlgK
FlgD
FlhA
FlgN
cell
secreted
Increase in FlgK export with addition of arginine (%)
60
50
40
30
20
10
0
*
+
-
arginine

Figure 3

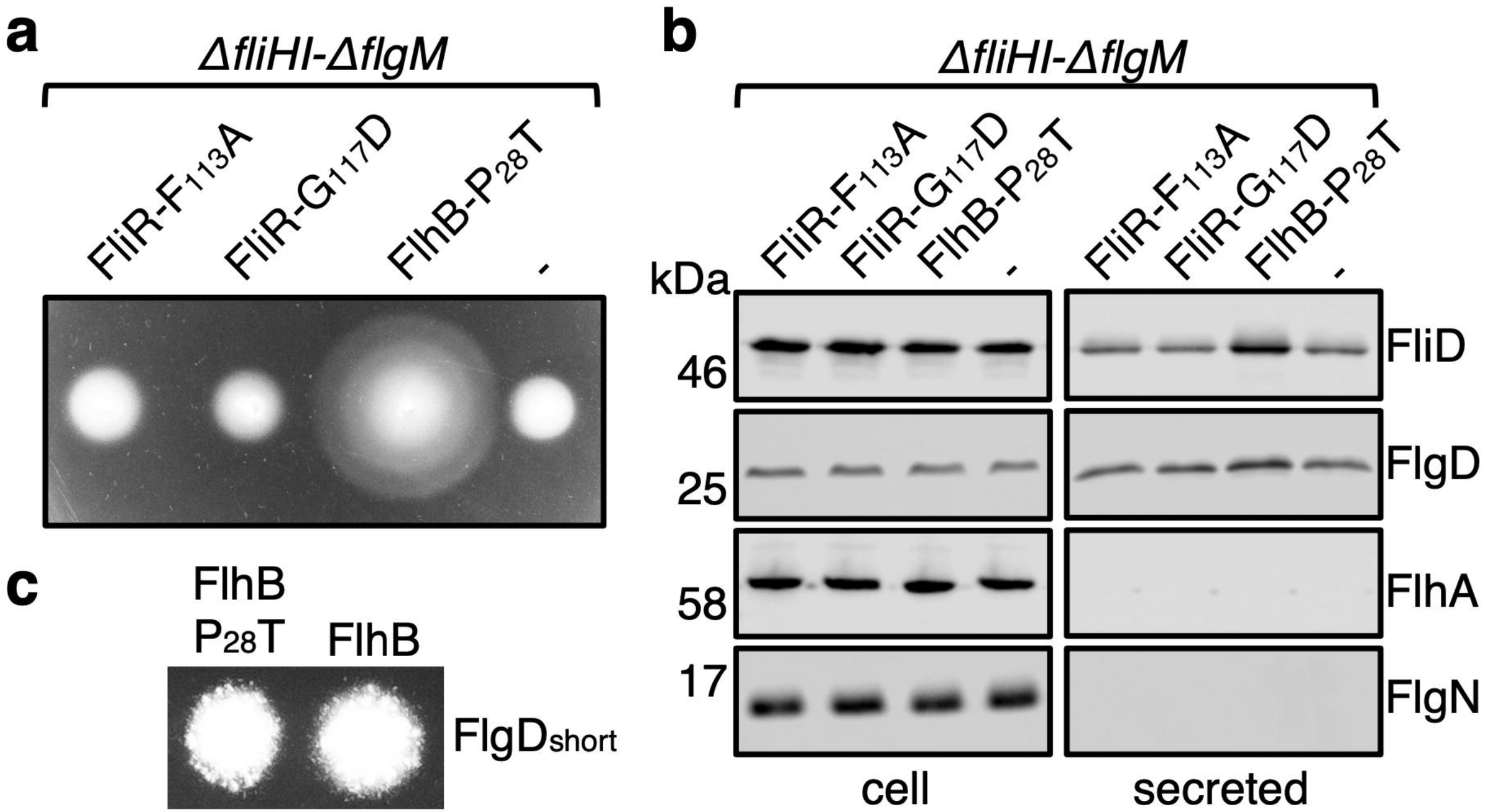
a
ΔfliHI-ΔflgM
FliR-F113A
FliR-G117D
FlhB-P28T
-
b
ΔfliHI-ΔflgM
FliR-F113A
FliR-G117D
FlhB-P28T
-
FliR-F113A
FliR-G117D
FlhB-P28T
-
kDa
46
25
58
17
FliD
FlgD
FlhA
FlgN
cell
secreted
c
FlhB
P28T
FlhB
FlgDshort

Figure 4

bioRxiv preprint doi: https://doi.org/10.1101/2021.01.17.426956; this version posted January 17, 2021. The copyright holder for this preprint (which was not certified by peer review) is the author/funder, who has granted bioRxiv a license to display the preprint in perpetuity. It is made available under aCC-BY-NC-ND 4.0 International license.

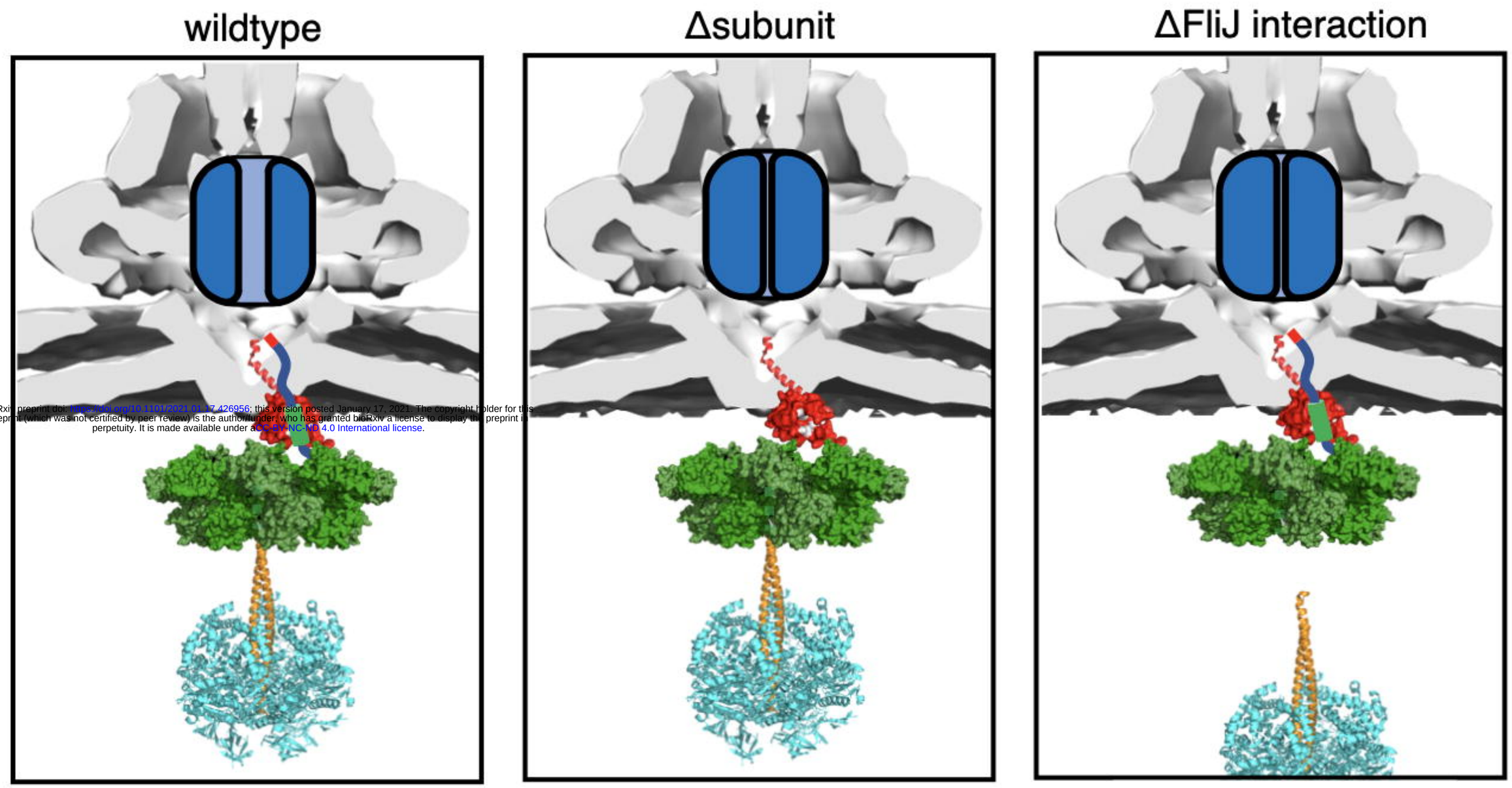

Figure 5